The ground state of an *XXZ* chain with asymmetric second-neighbour interactions

2007 J. Phys.: Condens. Matter 19 145226

(http://iopscience.iop.org/0953-8984/19/14/145226)

IOP PUBLISHING JOURNAL OF PHYSICS: CONDENSED MATTER

J. Phys.: Condens. Matter **19** (2007) 145226 (5pp) doi:10.1088/0953-8984/19/14/145226

The ground state of an XXZ chain with asymmetric second-neighbour interactions

M Nakane, Y Fukumoto and A Oguchi

Department of Physics, Faculty of Science and Technology, Tokyo University of Science, Noda, Chiba 278-8510, Japan

E-mail: yfuku@ph.noda.tus.ac.jp

Received 8 September 2006
Published 23 March 2007
Online at stacks.iop.org/JPhysCM/19/145226

Abstract

The ground state phase diagram of an XXZ chain with asymmetric second-neighbour interactions is studied. We first prove that this model has the doubly degenerate exact dimer ground state under some conditions. Then, by using the level spectroscopy method, we calculate the ground state phase diagram and find that the dependence of the dimer–fluid critical line on the asymmetric interactions is much stronger than those of the dimer–Néel critical line and the ferro-fluid first-order transition line. In order to understand this result, we analyse eigenvectors of the ground state and excitations characterizing each of phases, and show that only the doublet excitation can be used to detect the asymmetric interactions.

1. Introduction

The study of frustrated quantum spin systems is one of the central issues in condensed matter physics. The antiferromagnetic Heisenberg chain with second-neighbour couplings, or the railroad-lattice Heisenberg antiferromagnet, has received considerable attention for a long time, because it is simple but shows interesting ground state properties [1–3]. The ground state phase diagram of the XXZ chain with second-neighbour couplings was successfully obtained by Nomura and co-workers using the level spectroscopy (LS) method [4–7].

A similar model, the sawtooth-lattice Heisenberg antiferromagnet, has been studied by several authors [8–11]. This model was first introduced as a one-dimensional counterpart of the Kagomé-lattice Heisenberg antiferromagnet [8], and found to have a two-peak structure in the temperature dependence of the specific heat [8, 9]. Sen *et al* pointed out that this model is realized in $YCuO_{2.5}$ [10].

Recently, Chen *et al* introduced a Heisenberg chain with asymmetric second-neighbour couplings, which contains both of the models mentioned above as special cases [12, 13]. They used the Abelian bosonization to obtain a double-frequency sine–Gordon model, and asserted that the asymmetry leads to a new fixed point. However, Sarkar and Sen made an operator

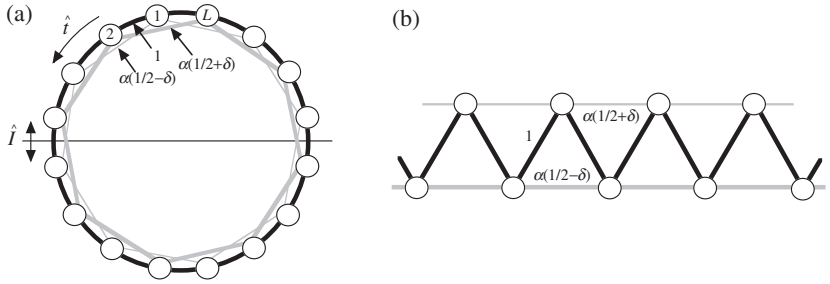

Figure 1. Schematic representations of (a) the XXZ chain with second-neighbour couplings and (b) the railroad lattice with asymmetric leg couplings, which is equivalent to the model in (a) and is reduced to the sawtooth lattice at $\delta = 1/2$. In (a), we define the translation operation $\hat{t}$ and the reflection operation $\hat{I}$, which are utilized in section 3.

product expansion of the terms in the bosonized Hamiltonian coming from the asymmetric couplings, and showed that those terms cancel each other and the new fixed point vanishes [14]. Their result was also checked numerically by Capriotti *et al* [15].

In this paper, we study the ground state phase diagram of an antiferromagnetic XXZ chain with asymmetric second-neighbour couplings,

$$H = \sum_{i=1}^{L} h_{i,i+1} + \alpha \sum_{i=1}^{L} \{1/2 + (-1)^i \delta\} h_{i,i+2}, \tag{1}$$

where $h_{i,j} = S_i^x S_j^x + S_i^y S_j^y + \Delta S_i^z S_j^z$, L denotes the total number of spins, and the periodic boundary condition $\boldsymbol{S}_{L+1} = \boldsymbol{S}_1$ is imposed (see figure 1(a)). We also confine ourselves to $0 \leqslant \alpha \leqslant 1$, $-1 \leqslant \Delta$ and $0 \leqslant \delta \leqslant 1/2$. This model is reduced to the railroad model at $\delta = 0$ and the sawtooth model at $\delta = 1/2$ (see figure 1(b)) [12, 13]. The main purpose of this work is to study how phase boundaries in the α–Δ plane depend on the asymmetry parameter δ.

2. Basic properties

We begin with proving that the dimer states,

$$\Psi_1 = [1,2][3,4]\cdots[L-1,L] \qquad \text{and} \qquad \Psi_2 = [2,3][4,5]\cdots[L,1] \tag{2}$$

with $[i,j] = (|\uparrow_i \downarrow_j\rangle - |\downarrow_i \uparrow_j\rangle)/\sqrt{2}$, are the ground state of our model for $\alpha = 1$ and $\Delta \geqslant -1/2$, following reference [16]. For this purpose, we rewrite the Hamiltonian with $\alpha = 1$ as follows:

$$H_{\alpha=1} = \sum_{l=1}^{L/2} h_l^{\text{plaq}}, \tag{3}$$

where $h_l^{\text{plaq}} = h_{2l,2l+1} + (1/2-\delta)(h_{2l-1,2l} + h_{2l-1,2l+1}) + (1/2+\delta)(h_{2l+1,2l+2} + h_{2l,2l+2})$. The minimum eigenvalue of h_l^{plaq} is $e_{\text{p}} = -(2+\Delta)/4$ for $\Delta \geqslant -1/2$ or $e_{\text{p}} = 3\Delta/4$ for otherwise. Thus the ground state energy, E_{g}, of $H_{\alpha=1}$ satisfies $E_{\text{g}} \geqslant e_{\text{p}} L/2$. The energy of the dimer state is $-(2+\Delta)L/8$, which proves the existence of the exact dimer ground state for $\alpha = 1$ and $\Delta \geqslant -1/2$. On the other hand, the ground state for $\Delta < -1/2$ is the ferromagnetic state whose energy is $3\Delta L/8$.

Next, we use the Abelian bosonization to get insight into the ground state phase diagram. The resultant continuum model is given by

$$H = \frac{a}{2\pi} \int \mathrm{d}x \left[A(\partial_x \phi)^2 + B(\pi \Pi)^2 \right] - C \int \frac{\cos 4\phi}{(2\pi a)^2}, \tag{4}$$

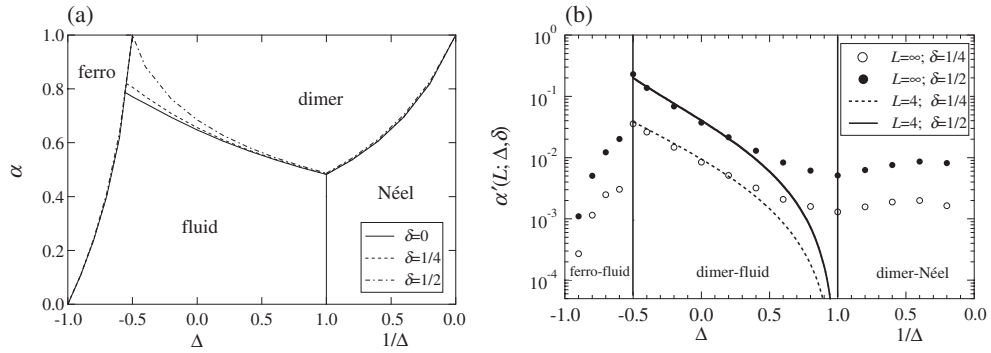

Figure 2. (a) Ground phase diagram in the $\alpha-\Delta$ plane for $\delta = 0, 1/4$ and $1/2$ in the thermodynamic limit $L = \infty$, and (b) plot of $\alpha'(L;\Delta,\delta) = \alpha_c(L;\Delta,\delta) - \alpha_c(L;\Delta,0)$ as a function of Δ for $L = \infty$ (markers) and $L = 4$ (lines).

where a is the lattice spacing, and

$$A = 1 + \frac{3\Delta}{\pi} + \frac{\alpha(6+\Delta)}{2\pi}, \tag{5}$$

$$B = 1 - \frac{\Delta}{\pi} - \frac{\alpha(2-\Delta)}{2\pi}, \tag{6}$$

$$C = a\left(\Delta - \frac{\alpha(2+\Delta)}{2}\right). \tag{7}$$

As pointed out by Sarkar and Sen [14], the continuum model is independent of the asymmetry parameter δ. Therefore, it is expected that phase boundaries in the ground state phase diagram do not depend on δ very much. In fact, numerical studies on the Heisenberg point $\Delta = 1$ by Capriotti *et al* showed that the position of the tricritical point depends on δ just slightly [15].

3. Ground state phase diagram

We employ the LS method to get the phase diagram in the α–Δ plane [4]. There exist fluid, Néel, dimer and ferromagnetic states in the ground state phase diagram. In the LS method, the fluid–dimer (Néel–dimer) transition point is determined as a crossing point of energies of doublet (Néel) and dimer excitations [4]. The point of the first-order transition to the ferromagnetic state is determined as an energy crossing point of the ferromagnetic state and the ground state in the $S^z_{\rm tot} = 0$ sector. For fixed values of L, Δ and δ, we calculate numerically the energy levels as functions of α to get an energy crossing point $\alpha_c(L;\Delta,\delta)$. An extrapolation to the thermodynamic limit $L = \infty$ is made through $\alpha_c(L;\Delta,\delta) = \alpha_c(\infty;\Delta,\delta) + \text{const.} \times L^{-2}$, where finite size data for $L = 12, 16, \ldots, 28$ are used. The extrapolation is rather satisfactory, and the resultant ground state phase diagram is shown in figure 2(a). We find that the dependence of the Néel–dimer transition line on the asymmetric parameter δ is quite slight, which is consistent with the naive expectation based on the bosonized Hamiltonian. We also find that the line of transition to the ferromagnetic state is almost independent of δ. However, the δ dependence of the fluid–dimer transition line is increasingly pronounced as Δ decreases. In order to see the δ dependences of those transition lines quantitatively, we define $\alpha'(L;\Delta,\delta) = \alpha_c(L;\Delta,\delta) - \alpha_c(L;\Delta,0)$. We show $\alpha'(\infty;\Delta,\delta)$ as a function of Δ in figure 2(b). Roughly speaking, the δ dependence of the fluid–dimer transition line for $\Delta<0$ is ten times that of other transition lines.

In order to understand the δ dependence of the transition lines, we turn to analysis of the eigenvectors. We here use the translation operation $\hat{t}$, the reflection operation $\hat{I}$, which are defined in figure 1(a), and the spin inversion operation $\hat{T}$. The eigenvalues of $\hat{t}$, $\hat{I}$ and $\hat{T}$ are written as $t = \mathrm{e}^{ik}$, I and T below. For $\delta = 0$, it is known that the ground state is in an $S^z_{\mathrm{tot}} = 0$ subspace with $(T, k, I) = (1, 0, 1)$, the dimer excitation is in that with $(1, \pi, 1)$, and the Néel excitation is in that with $(-1, \pi, -1)$. Operation of $\delta \sum_i (-1)^i h_{i,i+2}$ on basis functions with $(T, k, I) = (1, 0, 1)$, $(1, \pi, 1)$ or $(-1, \pi, -1)$ yields basis functions with $(T, k, I) = (1, \pi, -1)$, $(1, 0, -1)$ or $(-1, 0, 1)$. Thus, for $\delta > 0$, the ground state eigenvector, $|\Psi_{\mathrm{gs}}\rangle$, the eigenvector of the dimer excitation, $|\Psi_{\mathrm{dimer}}\rangle$, and that of the Néel excitation, $|\Psi_{\mathrm{Neel}}\rangle$, are written as follows:

$$|\Phi_{\mathrm{gs}}\rangle = |\phi_{1,0,1}\rangle \cos\theta_{\mathrm{gs}} + |\phi_{1,\pi,-1}\rangle \sin\theta_{\mathrm{gs}}, \tag{8}$$

$$|\Phi_{\mathrm{dimer}}\rangle = |\phi_{1,\pi,1}\rangle \cos\theta_{\mathrm{dimer}} + |\phi_{1,0,-1}\rangle \sin\theta_{\mathrm{dimer}}, \tag{9}$$

$$|\Phi_{\mathrm{Neel}}\rangle = |\phi_{-1,\pi,-1}\rangle \cos\theta_{\mathrm{Neel}} + |\phi_{-1,0,1}\rangle \sin\theta_{\mathrm{Neel}}, \tag{10}$$

where $|\phi_{T,k,I}\rangle$ represents a unit vector in the (T, k, I) subspace of $|\Phi_{\mathrm{gs}}\rangle$, $|\Phi_{\mathrm{dimer}}\rangle$ or $|\Phi_{\mathrm{Neel}}\rangle$ and we choose $0 \leqslant \theta \leqslant \pi/2$. (We hereafter call θ the 'mixing parameter'.) As for the doublet excitation, it is known that the symmetry of the doublet excitation is characterized by $(S^z_{\mathrm{tot}}, k, I) = (1, \pi, -1)$ when $\delta = 0$. Operation of $\delta \sum_i (-1)^i h_{i,i+2}$ on those basis functions yields basis functions with $(1, 0, 1)$. We can write the eigenvector of the doublet excitation for $\delta > 0$ as

$$|\Phi_{\mathrm{doublet}}\rangle = |\varphi_{1,\pi,-1}\rangle \cos\theta_{\mathrm{doublet}} + |\varphi_{1,0,1}\rangle \sin\theta_{\mathrm{doublet}}, \tag{11}$$

where $|\varphi_{S^z_{\mathrm{tot}},k,I}\rangle$ is a unit vector in the $(S^z_{\mathrm{tot}}, k, I)$ subspace of $|\Phi_{\mathrm{doublet}}\rangle$.

Because the LS method is known to give accurate results even for small size systems, we first look into the LS analysis of an $L = 4$ cluster. For the $L = 4$ cluster, we can obtain the mixing parameters analytically as follows:

$$\theta_{\mathrm{gs}} = \theta_{\mathrm{dimer}} = \theta_{\mathrm{Neel}} = 0, \qquad \theta_{\mathrm{doublet}} = \tan^{-1}\left(\frac{\sqrt{1 + [\alpha\delta(1-\Delta)]^2} - 1}{\alpha\delta(1-\Delta)}\right), \tag{12}$$

which tells us that only the doublet excitation is affected by the asymmetric interactions. As for the δ dependence of the phase boundaries, we obtain

$$\alpha'_{L=4}(\Delta, \delta) = \begin{cases} \dfrac{2}{3+\Delta}\left(\dfrac{1}{\sqrt{1 - \left[\frac{2\delta(1-\Delta)}{3+\Delta}\right]^2}} - 1\right) & \text{for dimer–fluid} \\ 0 & \text{for otherwise,} \end{cases} \tag{13}$$

which gives the solid and dashed lines in figure 2(b).

Comparing the result for $L = 4$ with that for $L = \infty$ in figure 2(b), we find that the LS analysis for the $L = 4$ cluster captures the qualitative nature of the present system, and thus we expect that only $\theta_{\mathrm{doublet}}$ can be large even for larger clusters. To check this point, we calculate the mixing parameter as a function of δ for an $L = 12$ cluster at two points near phase boundaries, $(\Delta, \alpha) = (-0.5, 0.9)$ and $(1/\Delta, \alpha) = (0.5, 0.7)$. The results are shown in figure 3. For $(\Delta, \alpha) = (-0.5, 0.9)$, which is near the dimer–fluid transition line, we find that $\theta_{\mathrm{gs}}, \theta_{\mathrm{dimer}}, \theta_{\mathrm{Neel}} \ll \theta_{\mathrm{doublet}}$ as expected. For $(1/\Delta, \alpha) = (0.5, 0.7)$, which is near the dimer–Néel transition line, we find all mixing parameters are small. These calculated results indicate that the pronounced δ dependence of the dimer–fluid transition line is originating from the fact that only the doublet excitation suffers from large mixing due to the asymmetric interactions. A more comprehensive study of eigenvectors is now proceeding. The results, together with details of our numerical calculations, will be reported in a separate publication.

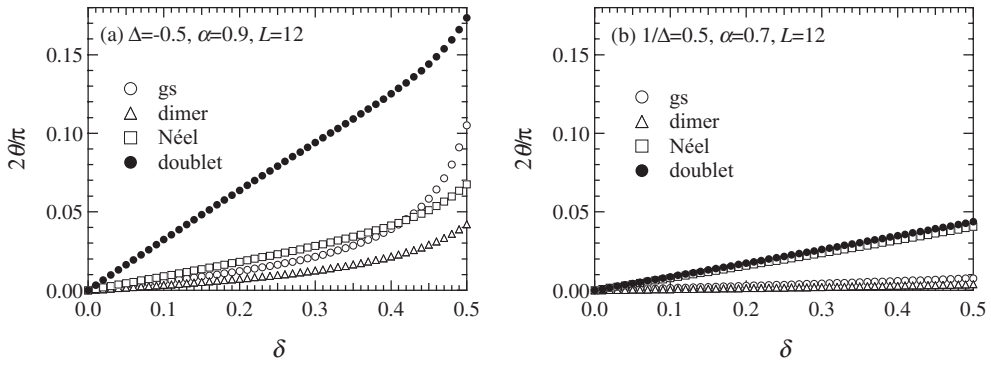

Figure 3. Mixing parameters θ as a function of δ for (a) $(\Delta, \alpha) = (-0.5, 0.9)$ and (b) $(1/\Delta, \alpha) = (0.5, 0.7)$. The system size is $L = 12$.

4. Summary

In summary, motivated by the fact that the bosonized Hamiltonian contains no terms coming from the asymmetry in the XXZ model with asymmetric second-neighbour couplings, we have studied the ground state phase diagram by using the LS method. Then, we found that the dependence of the fluid–dimer transition line on the asymmetry parameter δ is much greater than that of other transition lines. The distinct δ dependence of the fluid–dimer transition line can be interpreted as follows: the doublet excitation is a spin wave propagating in the quasi-long range ordered state, so this excitation can be affected by the short wavelength part of the Hamiltonian, such as the asymmetry in the second-neighbour couplings. It is worth mentioned that the triplet excitations, which are low-lying excitations in the dimer phase, can also detect the asymmetric part, like the doublet excitation. Thus, the triplet excitation gap in the dimer phase depends on δ [13]. However, our result indicates that the vanishing point of the gap, which should agree with a level crossing point between dimer and Néel excitations, is almost independent of δ.

References

[1] Majumdar C K and Ghosh D K 1969 *J. Math. Phys.* **10** 1388
[2] Majumdar C K and Ghosh D K 1969 *J. Math. Phys.* **10** 1399
[3] Haldane F D M 1982 *Phys. Rev.* B **25** 4925
[4] Nomura K and Okamoto K 1994 *J. Phys. A: Math. Gen.* **27** 5773
[5] Nomura K 1995 *J. Phys. A: Math. Gen.* **28** 5451
[6] Inoue H and Nomura K 1999 *Phys. Lett.* A **262** 96
[7] Hirata S and Nomura K 2000 *Phys. Rev.* B **61** 9453
[8] Kubo K 1993 *Phys. Rev.* B **48** 10552
[9] Otsuka H 1995 *Phys. Rev.* B **51** 305
[10] Sen D, Shastry B S, Walstedt R E and Cava R 1996 *Phys. Rev.* B **53** 6401
[11] Blundell S A and Núñez-Regueiro M D 2003 *Eur. Phys. J.* B **31** 453
[12] Chen S, Büttner H and Voit J 2001 *Phys. Rev. Lett.* **87** 087205
[13] Chen S, Büttner H and Voit J 2003 *Phys. Rev.* B **67** 054412
[14] Sarkar S and Sen D 2002 *Phys. Rev.* B **65** 172408
[15] Capriotti L, Becca F, Sorella S and Parola A 2003 *Phys. Rev.* B **67** 172404
[16] Shastry B S and Sutherland B 1981 *Phys. Rev. Lett.* **47** 964